Viscosity-Dependent Fluorescence Decay of the GFP Chromophore in Solution Due to Fast Internal Conversion

Andreas D. Kummer,*,† Christian Kompa,† Haruki Niwa,‡ Takashi Hirano,‡ Satoshi Kojima,‡ and Maria Elisabeth Michel-Beyerle*,†

Institut für Physikalische und Theoretische Chemie, Technische Universität München, 85748 Garching, Germany, and Department of Applied Physics and Chemistry, The University of Electro-communications, Chofu, Tokyo 182-8585, Japan

Received: December 31, 2001; In Final Form: April 29, 2002

Time-resolved fluorescence measurements at 275 K show that the excited-state lifetime of a model chromophore of the green fluorescent protein (GFP) substantially increases from subpicoseconds in low-viscosity solvents such as ethanol ($\eta = 1.7$ cP) to 30 ps in glycerol ($\eta = 9.9 \times 10^3$ cP) and reaches 2.1 ns in glycerol glass at 150 K. At high temperatures the similarity of excited-state decay and ground-state recovery kinetics indicates internal conversion being responsible for the short fluorescence lifetimes. Their viscosity dependence reflects on a motion with a considerable amplitude that is damped by viscous drag and outweighs thermal activation as is concluded from measurements at different temperatures. In solution the neutral and the anionic forms of the model chromophore are similarly nonfluorescent in contrast to wild-type GFP and mutants where the deprotonated form is hardly undergoing internal conversion. Thus, the protein selectively restricts motional degrees of freedom of the chromophore in specific protonation states.

1. Introduction

The green fluorescent protein (GFP) from the jellyfish *Aequorea victoria* is widely used as a noninvasive marker for gene expression and protein localization.[1] Tightly fixed inside the can-shaped protein,[2,3] its chromophore exhibits a high fluorescence quantum yield of ≈0.8[1,4] but emission is lost upon protease digestion or heat denaturation and, most interestingly, is weak in some important blue- and red-shifted mutants.[5−7] Elucidation of the radiationless deactivation mechanisms in these "nonfluorescing mutants" is of central importance for the development of mutagenetic strategies which result in color changes while maintaining a high quantum yield of fluorescence.

As the predominant process for the loss of fluorescence intensity in certain GFP mutants internal conversion has been envisaged.[5,6,8,9] Internal conversion rates have been shown to depend on the protonation states of the chromophore.[5] To gain more insight into the spectrum of parameters contributing to this decay pathway two lines of experiments have currently been explored: (i) fluorescence lifetime measurements on specific single-site mutants with defined changes in hydrogen bond stabilization toward rotational motion within the chromophore[7] and (ii) detailed steady-state and time-resolved spectroscopic studies of a model chromophore in solution.[10−12]

The present paper is devoted to the second approach. It is based on a model compound for the GFP chromophore (compound **1** in Scheme 1) which is formed by a tyrosyl residue attached via the combination of a single and a double bond to an imidazolone ring.[13] In the context of this paper we attribute no relevance to the acetate group attached to the heterocycle.

SCHEME 1: Model Compound 1, Ethyl 4-(4-Hydroxyphenyl)methylidene-2-methyl-5-oxo-1-imidazolacetate

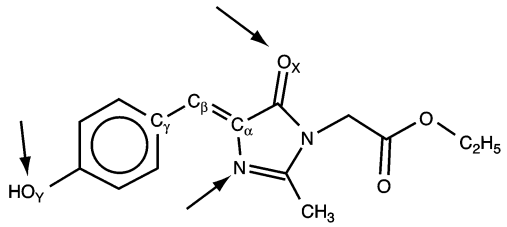

Compound **1** shows no significant fluorescence in solution at high temperatures but becomes highly fluorescent in low-temperature organic glasses, e.g., in ethanol at 77 K.[13] These observations were interpreted in terms of "a competition between the isomerization of the *exo*-methylene double bond and fluorescence emission."[13]

Studies of this model chromophore provide essentially three advantages which help to further establish the validity of the concept of internal conversion operative in some weakly fluorescent GFP mutants and to define the important parameters. (i) In the absence of suitable redox partners electron-transfer quenching can be ruled out a priori as the origin of the fluorescence loss. Although there is no evidence for this mechanism, it may in principle contribute to short fluorescence lifetimes in mutants in which aromatic amino acids (e.g., tryptophane and tyrosine) are in close vicinity of the excited chromophore. (ii) In solution experiments the parametric change of the protonation state of the model chromophore is feasible by adjustment of the proton concentration. This parameter is of special interest since the experimental results may be compared to quantumchemical calculations which predict the influence of protonation on the activation barrier for rotation. (iii) In terms of the macroscopic viscosity which is known to

* Corresponding authors. Fax: +49-89-289-13026. E-mail for Andreas Kummer: Andreas.Kummer@ch.tum.de. E-mail for Maria Elisabeth Michel-Beyerle: Michel-Beyerle@ch.tum.de.

† Institut für Physikalische und Theoretische Chemie.

‡ Department of Applied Physics and Chemistry.

10.1021/jp014713v CCC: $22.00
Published on Web 07/10/2002

affect rotational motion in molecules with exocyclic double bonds as, e.g., the stilbenes,[14−16] the influence of this parameter on the fluorescence of the model chromophore can be put to test by variation of either solvent and/or temperature.

On the basis of comparative femtosecond time-resolved measurements indicative of internal conversion as the origin of short lifetimes under low-viscosity conditions we explored the sensitivity of excited-state lifetimes to changes in the macroscopic viscosity and the role of temperature. For solubility reasons polar solvents were chosen which provide a wide range of viscosities.

2. Materials and Methods

2.1. Sample Preparation. Model compound **1**, ethyl 4-(4-hydroxyphenyl)methylidene-2-methyl-5-oxo-1-imidazolacetate[13] was dissolved in ethanol, ethylene glycol, and glycerol to a concentration of 77, 73, and 79 μM, respectively. Particularly in the case of glycerol care was exercised to prevent absorption of water, which considerably would have altered the viscosity of the solution: A fresh charge of glycerol was used (H_2O < 0.1%), and the sample was kept sealed against air. The deprotonated form of model compound **1** was prepared by adding 1 vol % 0.1 M NaOH aqueous solution (value for the viscosity corrected accordingly).

2.2. Spectroscopic Measurements. *2.2.1. Steady-State Absorption and Fluorescence Measurements.* Steady-state absorption and fluorescence spectra were measured as previously described with ≤2.0 nm resolution.[17] A 1 mm path-length quartz cuvette was used in both spectrometers. Fluorescence was detected in a front-face geometry.

2.2.2. Picosecond Time-Resolved Fluorescence Measurements. Excitation light pulses at wavelengths between 364 and 432 nm were obtained by frequency-doubling either the output of a cavity dumped dye-laser (Coherent 701-CD) or a Ti:sapphire laser (Coherent MIRA) using a BBO crystal (for details see refs 6 and 17). Fluorescence kinetics were measured under magic angle conditions using two detection systems: (i) a femtosecond streak camera (Hamamatsu SYNCHROSCAN FESCA C6860, a demo unit kindly put at our disposal by Hamamatsu Photonics Deutschland GmbH) and (ii) time-correlated single-photon-counting (TCSPC). Using standard deconvolution procedures, lifetimes shorter (down to a third) than the fwhm of the apparatus response function (2 ps and 30−40 ps in case of (i) and (ii), respectively) were considered to have an ambiguity of a factor of 2. All other lifetimes carry an approximate error of <20%. Low-temperature measurements—steady-state as well as time-resolved—were performed using a continuous-flow cryostat (Leybold VSK 3−300) with liquid nitrogen. Steady-state absorption spectra were taken prior and after the measurements to check for possible sample degeneration during the experiments. A reference sample of the solvent alone was checked to make sure that the fluorescent impurity traces found in glycerol were too long-lived to be seen in the time-resolved measurements.

2.2.3. Femtosecond Time-Resolved Absorption Measurements. Femtosecond time-resolved transient absorption data were recorded in a one-color (λ = 390 nm) experiment using a pump-and-probe setup with an estimated time resolution of 150 fs described elsewhere in more detail.[6]

3. Results and Discussion

3.1. Steady-State Spectroscopy. In contrast to intact wild-type GFP, the absorption spectrum of model compound **1** in polar organic solvents is highly sensitive to pH. The possible protonation sites O_X, N, and O_Y are marked with arrows in Scheme 1. In the pure solvents studied here compound **1** is supposed to exist in its neutral form (HO_Y, N, O_X).[13,18] In ethanol (ϵ = 24.55) the corresponding main absorption band peaks at 372 nm (Figure 1). Presumably due to a slight dependence on the static dielectric constant ϵ of the solvent this maximum is red-shifted to 374 nm in ethylene glycol (ϵ = 37.7) and 376 nm in glycerol (ϵ = 42.5). We assume the minor absorption feature observed at 250 nm to correspond to the S0 → S2 transition of the neutral form of compound **1**.

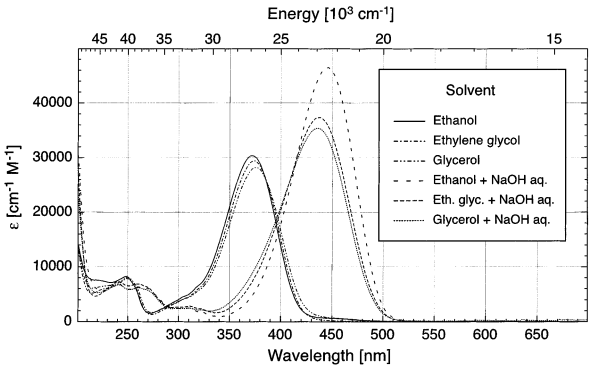

Figure 1. Room-temperature steady-state absorption spectra of model compound **1** in ethanol, ethylene glycol and glycerol with/without the addition of 1 vol % 0.1 M NaOH aq. Concentration of compound **1** = 77, 73, and 79 μM, respectively.

Raising the basicity of the solutions favors deprotonation and is supposed to lead to the anionic form (O_Y, N, O_X)$^-$.[13,18] In ethanol the peak position of the absorption band is now red-shifted to 446 nm (Figure 1). The corresponding values for ethylene glycol and glycerol are somewhat blue-shifted, to 438 and 436 nm, respectively. While the absorption spectrum of the neutral form is only slightly sensitive to the temperature, a strong temperature dependence is observed for the anionic form, e.g., in ethanol. Here, lowering the temperature to 100 K leads to a blue-shift of 22 nm, in contrast to a red shift of only 2 nm in the case of the neutral form.

At room temperature weak fluorescence can be detected of the neutral as well as of the anionic form in glycerol, while for ethanol and ethylene glycol almost only Raman scattering can be seen in the fluorescence emission spectra. However, upon the lowering of the temperature near to or below, the glass-transition point of each solvent strong fluorescence developes. In general, the emission spectra are broad and unstructured with the exception of compound **1** in ethanol were a vibronic progression begins to emerge at 100 K (data not shown). The fluorescence intensity reaches its maximum in the range (450 ± 25) nm and (490 ± 25) nm for the neutral and the anionic forms, respectively. The exact peak position and the shape of the fluorescence spectrum is dependent not only on solvent and temperature but also on excitation wavelength, the latter effect being more pronounced for the neutral than for the anionic form (e.g., in glycerol at 80 K, see Figure 2). Closer inspection of the neutral form reveals more details: While excitation at various wavelengths in the blue wing of the absorption band leads to fluorescence with an almost invariable fluorescence peak position, excitation in the red wing alters the shape of the fluorescence spectrum considerably (Figure 2), and the fluorescence peak shifts to the red with increasing excitation wavelength. In the case of the anionic form, changes in the shape of the emission spectrum are less prominent and a simple red shift with increasing excitation wavelength predominates.

The corresponding excitation spectra are broad and featureless as well—again with the exception of compound **1** in ethanol at

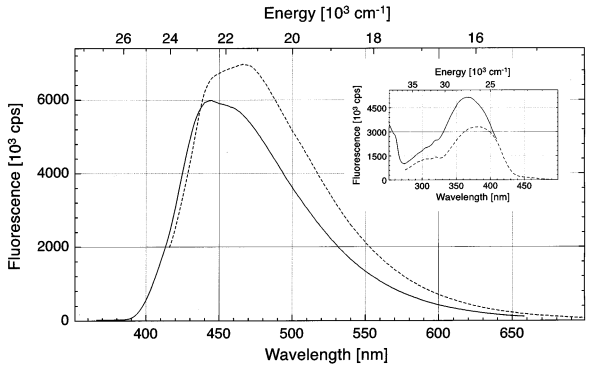

Figure 2. Steady-state fluorescence emission spectra of model compound **1** in glycerol, 79 μM at 80 K. $\lambda_{exc} = 345$ nm (solid line) and 405 nm (dashed line). Inset: Corresponding excitation spectra with $\lambda_{det} = 420$ nm (solid line) and 510 nm (dashed line).

100 K. In all other samples the single excitation peak is gradually blue-shifted with decreasing emission wavelength (see inset Figure 2). It is interesting to note that the peak wavelengths of the vibronic bands seen in the ethanol sample at 100 K are not dependent on emission wavelength. Only the relative intensities of the different peaks change, yielding the overall blue shift observed in the other samples as well.

3.2. Femtosecond/Picosecond Time-Resolved Spectroscopy. The data of picosecond time-resolved fluorescence measurements in different alcohols and at different temperatures are listed in Table 1 (see also Figure 3). The fluorescence decay traces of the model compound in glycerol at all temperatures, and in the other solvents at temperatures at which high viscosities prevail, are nonexponential. In a given sample at a fixed temperature there is, in general, a trend to slightly shorter lifetimes with increasing emission wavelength. Together with the dependency of fluorescence spectra on excitation wavelength (see above), the spectral dependence of fluorescence lifetimes and the nonexponential decay pattern indicate dispersive kinetics reflecting static heterogeneity of the chromophore in specificly structured solvent cages and/or the presence of a mixture of *E*- and *Z*-isomers. This is equivalent with the notion that fluctuations between different conformations occur on time scales longer than the fluorescence lifetime.

An exception to the nonexponential decay pattern is given by the model compound in glycerol glass: At 150 K, the fluorescence lifetime is 2.1 ns for neutral and 3.0 ns for anionic compound **1** and the fluorescence decay is almost monoexponential. Interestingly, the decay traces in this case clearly exhibit a rise component of about 150−200 ps with a large amplitude, indicating that a large part of the emitting species is generated after excitation. This effect is tentatively explained by a conformational change in the excited state. With respect to the structure of compound **1** (Scheme 1) the lifetime of solute/solvent hydrogen bonds which may affect the fluorescence quantum yield might be reflected in the rise dynamics.[19]

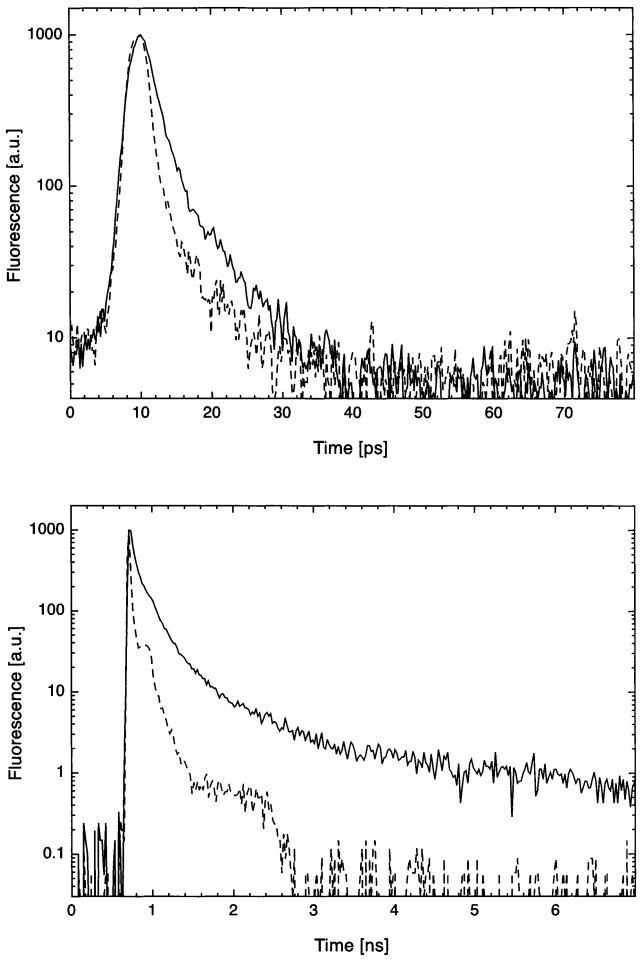

Figure 3. Fluorescence traces of model compound **1** in ethylene glycol (73 μM, upper part) and glycerol (79 μM, lower part) at 275 K (solid lines). λ_{exc}, λ_{det} as given in Table 1. Instrument response function (dashed line) with 2 ps fwhm (upper part) and 28 ps fwhm (lower part), respectively.

TABLE 1: Fit Results of Fluorescence Measurements at Selected Temperatures for Model Compound 1 in Ethanol, Ethylene Glycol, and Glycerol with/without the Addition of 1 vol % 0.1 M NaOH aq[a]

solvent	T [K]	λ_{exc} [nm]	λ_{det} [nm]	t_1	A_1 [%]	t_2	A_2 [%]	t_3	A_3 [%]	t_4	A_4 [%]	$t_{1/e}$
ethanol	275[b]	397	515	0.6 ps	99.9[c]	0.32 ns	0.1					0.6 ps
	200[b]	397	515	1.0 ps	100[c]							1.0 ps
	100	364	515	39 ps	47.6	0.31 ns	25.6	1.2 ns	17.6	2.6 ns	9.1	0.20 ns
ethylene glycol	275[b]	397	515	1.3 ps	96.6[c]	6.1 ps	3.4					1.3 ps
glycerol	275	364	515	20 ps	69.4	76 ps	27.1	0.35 ns	3.4	2.7 ns	0.1	30 ps
ethanol + NaOH aq.	275[b]	432	530	0.8 ps	94.5[c]	4.2 ps	5.5					0.9 ps
	200[b]	432	530	1.0 ps	88.3	6.0 ps	11.7					1.2 ps
	100	432	530	13 ps	25.3	0.15 ns	28.4	0.73 ns	12.7	2.2 ns	33.5	0.41 ns
ethylene glycol + NaOH aq	275[b]	432	530	1.8 ps	70.6	13 ps	29.4					2.9 ps
glycerol + NaOH aq	295	432	530	8.4 ps	65.2	61 ps	31.3	0.22 ns	3.5			16 ps
	275	432	530	14 ps	45.8	87 ps	38.1	0.36 ns	11.8	0.91 ns	4.3	51 ps
	250	432	530	24 ps	36.4	0.15 ns	34.6	0.73 ns	16.6	1.9 ns	12.4	0.16 ns

[a] Concentration of compound **1** = 77, 73, and 79 μM, respectively. Amplitudes are normalized to 100%. [b] Measured with Hamamatsu SYNCHROSCAN FESCA C6860. [c] The monoexponentiality of this measurement has to be taken with caution since the signal level was very low, and the fluorescence lifetime was in the range of the fwhm of the instrument response function.

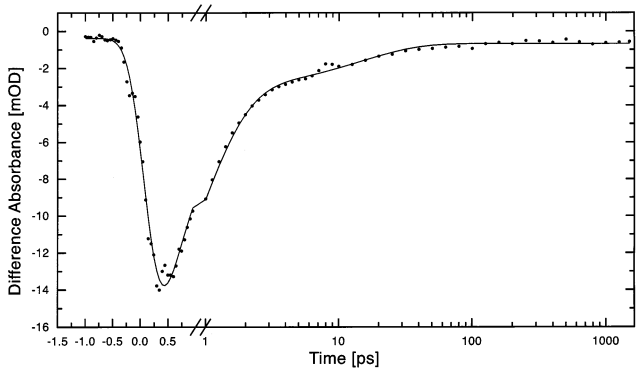

Figure 4. Model compound **1** in ethanol, 77 μM at room temperature. Transient absorption, pump and probe at 390 nm.

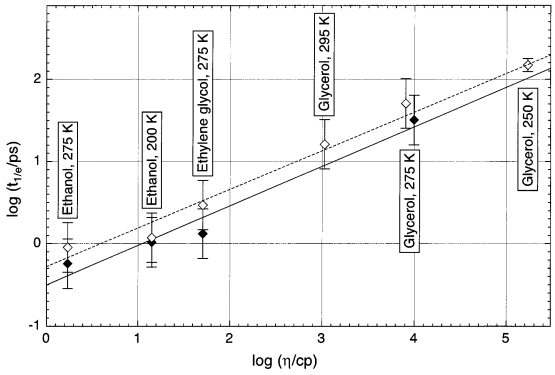

Figure 5. Model compound **1** in ethanol (77 μM), ethylene glycol (73 μM), and glycerol (79 μM) at selected temperatures. Fluorescence lifetime $t_{1/e}$ vs macroscopic viscosity η under neutral (closed symbols, solid line) and basic (open symbols, dashed line) condition. λ_{exc}, λ_{det} as given in Table 1. Values for η as found in the literature[29−31] and corrected for the addition of 1 vol % 0.1 M NaOH aq where applicable. For both conditions regression analysis yields a linear dependence with a slope of 0.5 leading to the expression $t_{1/e}/\text{ps} = a\,(\eta/\text{cP})^{1/2}$ with a = 0.3 and 0.5 for neutral and anionic compound **1**, respectively.

In ethanol at 275 K, the fluorescence-decay time constant of 0.57 ps was at the limit of the time resolution of the streak camera (FESCA, see Section 2.2.2) and is consistent with the observation that in steady-state measurements no fluorescence is detectable. To establish internal conversion as the predominant mechanism responsible for short fluorescence lifetimes, the ground-state recovery dynamics of compound **1** have been investigated. A single-color transient absorption measurement (pump and probe at 390 nm) monitoring the ground-state absorption of the protonated form of compound **1** in ethanol at room temperature shows that after the initial bleaching of the sample the ground-state absorption is recovered. The kinetic trace in Figure 4 can be fitted with two time constants, a 700 fs component with an amplitude of −19 mOD and a 14.6 ps component with a small amplitude of −2.6 mOD. These data from transient absorption are well within the error bars of the fluorescence measurement. The similarity of ground-state recovery and excited-state decay kinetics strongly supports the notion of internal conversion as the predominant mechanism.

Recently, ultrafast one-color pump−probe spectroscopy was employed to measure the ground-state recovery kinetics of a model compound similar to compound **1** in a variety of alcohol solutions.[11,12] The fast recovery times were compared to the low fluorescence quantum yields derived from steady-state measurements and interpreted as radiationless losses due to internal conversion. Essentially no dependence on the macroscopic viscosity η of the solvents was reported in the range $0.5 \le \eta \le 16$ cP. We extended the viscosity range by several orders of magnitude and observed a pronounced dependence of the fluorescence lifetime on solvent viscosity. At 275 K the results summarized in Figure 5 and in Table 1 show an increase of the fluorescence-decay time from subpicoseconds for ethanol (η = 1.7 cP) to 1.3 ps for ethylene glycol (η = 50.9 cP) and 30 ps for glycerol ($\eta = 9.9 \times 10^3$ cP). This pronounced increase in the excited-state lifetime of compound **1** dissolved in high-viscosity solvents and the nearly radiation limited decay time of a few nanoseconds observed in glycerol glass (see above) suggests that the nonradiative decay channel is coupled to a motion that requires more space than the free volume accessible to the moving components of the excited molecule. Rearrangement of the solvent cage is necessary and therefore, the motion is damped by viscous drag.

Compared to the neutral form of the model compound, the fluorescence lifetime of the anion is generally longer but only by a factor of less than three (Figure 5 and Table 1). This result is unexpected since in wild-type GFP and several mutants the difference in excited-state lifetime of the protonated and the deprotonated chromophore species is much more pronounced.[5,6] For instance, in the native protein the excited deprotonated chromophore is long-lived (3.3 ns) while for the protonated form the average time constant of internal conversion can be estimated to be in the range of 0.2 ns.[5] We note in passing that this time constant cannot be measured directly since the excited-state lifetime of the protonated chromophore is essentially determined by excited-state proton transfer occurring on the picosecond time scale.[17,20]

To explain the observation that neutral and anionic forms are similarly (non-) fluorescent in solution but exhibit a pronounced difference in internal conversion rate in the intact protein, one has to consider that in solution both the phenolic group and the imidazolone ring of the chromophore are free to rotate: in intact GFP the latter is rigidly attached to the protein backbone by two covalent bonds. This fixation together with the overall packing in the protein barrel might restrict selectively motional degrees of freedom of the chromophore. With the imidazolone ring fixed, rotation around the $C_\beta-C_\alpha$ bond would require a large-scale movement of the phenyl ring (Scheme 1) that leads to major steric conflicts with the rigid GFP environment. On the other hand rotation around the $C_\gamma-C_\beta$ bond is expected to be less perturbed by the protein surroundings because the phenyl ring is rotated around its own axis. Therefore, we suggest that in the anion rotation around $C_\beta-C_\alpha$ is energetically favored in solution and effectively hindered in the protein, while in the neutral form rotation around $C_\gamma-C_\beta$ leads to the observed radiationless losses in both solution and protein environment as well. The latter is furthermore supported by a recent study on single-site chromophore mutants of GFP in which the anion cannot be formed.[7] These blue-emitting variants were shown to be substantially more fluorescent when the distal aromatic ring is fixed to the surroundings via hydrogen bonds in such a way that rotation around $C_\gamma-C_\beta$ is suppressed, while a fixation that mainly affects the rotation around $C_\beta-C_\alpha$ was found to have only a minor influence on the radiationless losses of the neutral chromophore species.

Plotting the fluorescence lifetime $t_{1/e}$ at 275 K versus the macroscopic viscosity η on a double-logarithmic scale (Figure 5) reveals a linear dependence with a slope of 0.5 for the neutral as well as for the anionic form. A simple mathematical transformation leads to the expression $t_{1/e}/\text{ps} = a(\eta/\text{cP})^{1/2}$ with a = 0.3 and 0.5 for neutral and anionic compound **1**, respectively (a being a dimensionless constant of proportionality). Taking into account the measurements at other temperatures for which

viscosity data is at hand, this result is not altered significantly (Figure 5). At 100 K in supercooled ethanol the fluorescence lifetime reaches 0.2 ns in the case of the neutral and 0.4 ns in the case of the anionic form. Extrapolation of the observed dependency yields a value for the macroscopic viscosity of $(5-7) \times 10^5$ cP. For ethanol near the glass-transition temperature T_g we could not find viscosity data in the literature. However, a qualitative comparison for instance with propanol[21] supports the assumption that for glass forming liquids near T_g this value is rather too low than overestimating the actual macroscopic viscosity of the sample. Therefore, the increase in the lifetime of the excited state can be explained exclusively on the basis of viscosity changes and no thermal activation of the process needs to be employed.

A similar nonlinear viscosity dependence was also reported in triphenyl-methane dyes, e.g., crystal violet,[22−26] and stilbenes[14−16] in high-viscosity solvents ($\eta > 10$ cP). The nonlinear viscosity dependence was interpreted in terms of dynamics limited by diffusive large amplitude motion either on a barrierless potential as in the case of the triphenyl-methane dyes or with a small internal potential energy barrier as in the case of the stilbenes. While at high viscosities this nonlinear dependence is well-established, in the low-viscosity range a linear dependency of the excited-state decay time on η was found for crystal violet in short-chain *n*-alcohol solvents.[24,25] This linear dependency at low viscosities is predicted by the theory of Bagchi−Fleming−Oxtoby (BFO)[27] provided that the following conditions hold: (i) the motion leading to internal conversion has to proceed on a barrierless potential and (ii) a pinhole sink function is connecting the excited states and ground states. However, for the case of a nonlocal sink function (or a nonzero activation barrier) BFO postulate a nonlinear viscosity dependence even in the low-viscosity regime. Furthermore, in cases of very low solvent viscosity application of BFO is hampered by inertial effects and the excited-state decay rates may be overestimated.[28]

Our low-viscosity data falls within the sublinear viscosity dependence we derived above. In this context it is important to stress that the macroscopic viscosity is a solvent-specific property and therefore, in many if not most cases is only a very limited measure for the actual solute/solvent-specific microfriction experienced by the rotating portion of the excited molecule under consideration. Especially in the case of compound **1** in alcohol solutions, hydrogen bonding between the solvent and the solute must be considered rendering the system particularly sensitive to solvent/solute interactions.

4. Conclusions

Time-resolved measurements show that the fluorescence of a GFP model chromophore (compound **1**) is explicitly coupled to the macroscopic viscosity of the solvent and a sublinear dependence of the fluorescence lifetime $t_{1/e} \propto \eta^{1/2}$ is observed. Similar kinetics of excited-state decay and ground-state recovery support internal conversion as the predominant mechanism responsible for the loss of fluorescence. At 275 K the excited-state lifetime increases from subpicosecond in low-viscosity solvents such as ethanol ($\eta = 1.7$ cP) to 30 ps in glycerol ($\eta = 9.9 \times 10^3$ cP) and reaches 2.1 ns in glycerol glass at 150 K. These results are interpreted in terms of the nonradiative decay channel being coupled to a motion with a considerable amplitude that is damped by viscous drag.

Measurements down to 100 K indicate that the dependence of fluorescence lifetime on viscosity outweighs thermal activation among other influences. Consequently, the dramatic increase in fluorescence quantum yield upon lowering the temperature reported for three GFP mutants[5,7] can be attributed to increased sterical restraints put forward on the chromophore by the surrounding protein rather than to thermal activation of the loss channel itself.

In contrast to the situation in wild-type GFP and mutants, the neutral and the anionic forms of compound **1** are similarly fluorescent in solution. This indicates that the protein selectively restricts motional degrees of freedom of the chromophore depending on its protonation state. The green emission of the deprotonated chromophore owes its high quantum yield to the attachment of the imidazolone ring to the protein backbone which effectively suppresses rotation around the $C_\beta-C_\alpha$ bond. In contrast, rotation of the distal aromatic ring around the $C_\gamma-C_\beta$ bond in the protonated form still seems to be possible in the protein at room temperature, since in some blue and yellow GFP mutants fast radiationless losses are observed.[5−7] In these mutants the excited-state lifetime of the protonated chromophore is almost as short as in solution. This view of motional freedom of the protonated chromophore is also supported by the dramatic increase of the excited-state lifetime to almost 1 ns upon fixation of the distal aromatic ring via hydrogen bonds in a specific blue mutant (Y66H).[7] In summary, high fluorescence quantum yields of wild-type GFP and its mutants can only be achieved by suppressing internal conversion of the chromophore via fine-tuning a combination of tight packing, two concerted covalent bonds to the backbone and hydrogen-bond fixation of the distal aromatic ring.

References and Notes

(1) Tsien, R. Y. *Annu. Rev. Biochem.* **1998**, *67*, 509.

(2) Yang, F.; Moss, L. G.; Phillips, G. N., Jr. *Nature Biotechnol.* **1996**, *14*, 1246.

(3) Ormö, M.; Cubitt, A. B.; Kallio, K.; Gross, L. A.; Tsien, R. Y.; Remington, S. J. *Science* **1996**, *273*, 1392.

(4) Morise, H.; Shimomura, O.; Johnson, F. H.; Winant, J. *Biochemistry* **1974**, *13*, 2656.

(5) Kummer, A. D.; Kompa, C.; Lossau, H.; Pöllinger-Dammer, F.; Michel-Beyerle, M. E.; Silva, C. M.; Bylina, E. J.; Coleman, W. J.; Yang, M. M.; Youvan, D. C. *Chem. Phys.* **1998**, *237*, 183.

(6) Kummer, A. D.; Wiehler, J.; Rehaber, H.; Kompa, C.; Steipe, B.; Michel-Beyerle, M. E. *J. Phys. Chem. B* **2000**, *104*, 4791.

(7) Kummer, A. D.; Wiehler, J.; Schüttrigkeit, T. A.; Berger, B. W.; Steipe, B.; Michel-Beyerle, M. E. *CHEMBIOCHEM* **2002**, *3*, 659.

(8) Voityuk, A. A.; Michel-Beyerle, M. E.; Rösch, N. *Chem. Phys. Lett.* **1998**, *296*, 269.

(9) Weber, W.; Helms, V.; McCammon, J. A.; Langhoff, P. W. *Proc. Natl. Acad. Sci. U.S.A.* **1999**, *96*, 6177.

(10) Kummer, A. D.; Michel-Beyerle, M. E. Conference on "Light-Induced Dynamics in Proteins"; April 2−6, 2001, Freising, Germany, Deutsche Forschungsgemeinschaft, Sonderforschungsbereich 533.

(11) Webber, N. M.; Litvinenko, K. L.; Meech, S. R. *J. Phys. Chem. B* **2001**, *105*, 8036.

(12) Litvinenko, K. L.; Webber, N. M.; Meech, S. R. *Chem. Phys. Lett.* **2001**, *346*, 47.

(13) Niwa, H.; Inouye, S.; Hirano, T.; Matsuno, T.; Kojima, S.; Kubota, M.; Ohashi, M.; Tsuji, F. I. *Proc. Natl. Acad. Sci. U.S.A.* **1996**, *93*, 13617.

(14) Sharafy, S.; Muszkat, K. A. *J. Am. Chem. Soc.* **1971**, *93*, 4119.

(15) Sun, Y. P.; Saltiel, J. *J. Phys. Chem.* **1989**, *93*, 8310.

(16) Schroeder, J.; Schwarzer, D.; Troe, J.; Vöhringer, P. *Chem. Phys. Lett.* **1994**, *218*, 43.

(17) Lossau, H.; Kummer, A.; Heinecke, R.; Pöllinger-Dammer, F.; Kompa, C.; Bieser, G.; Jonsson, T.; Silva, C. M.; Yang, M. M.; Youvan, D. C.; Michel-Beyerle, M. E. *Chem. Phys.* **1996**, *213*, 1.

(18) Voityuk, A. A.; Kummer, A. D.; Michel-Beyerle, M. E.; Rösch, N. *Chem. Phys.* **2001**, *269*, 83.

(19) Yu, J.; Berg, M. *Chem. Phys. Lett.* **1993**, *208*, 315.

(20) Chattoraj, M.; King, B. A.; Bublitz, G. U.; Boxer, S. G. *Proc. Natl. Acad. Sci. U.S.A.* **1996**, *93*, 8362.

(21) Ling, A. C.; Willard, J. E. *J. Phys. Chem.* **1968**, *72*, 1918.

(22) Magde, D.; Windsor, M. W. *Chem. Phys. Lett.* **1974**, *24*, 144.

(23) Hirsch, M. D.; Mahr, H. *Chem. Phys. Lett.* **1979**, *60*, 299.
(24) Sundstrom, V.; Gillbro, T.; Bergstrom, H. *Chem. Phys.* **1982**, *73*, 439.
(25) Ben-Amotz, D.; Harris, C. B. *J. Phys. Chem.* **1987**, *86*, 4856.
(26) Ben-Amotz, D.; Harris, C. B. *J. Phys. Chem.* **1987**, *86*, 5433.
(27) Bagchi, B.; Fleming, G. R.; Oxtoby, D. W. *J. Chem. Phys.* **1983**, *78*, 7375.
(28) Bagchi, B.; Singer, S.; Oxtoby, D. W. *Chem. Phys. Lett.* **1983**, *99*, 225.
(29) Weast, R. C., Ed. *CRC Handbook of Chemistry and Physics*; CRC Press, Inc.: Cleveland, Ohio, 1977.
(30) Litovitz, T. A.; Higgs, R.; Meister, R. J. *Chem. Phys.* **1954**, *22*, 1281.
(31) Segur, J. B.; Oberstar, H. E. *Ind. Eng. Chem.* **1951**, *43*, 2117.